

ASE FLOODWATER CLASSIFIER DEVELOPMENT FOR EO-1 HYPERION IMAGERY

Felipe Ip¹ (felipe@hwr.arizona.edu), J. M. Dohm¹, V. R. Baker¹, T. Doggett³, A. G. Davies², B. Castano², S. Chien², B. Cichy², R. Greeley³, R. Sherwood² ¹Dept. of Hydrology and Water Resources, University of Arizona, Tucson, AZ 85721, ²Jet Propulsion Laboratory, Pasadena, CA 91109-8099, ³Dept. of Geological Sciences, Arizona State University, Tempe, AZ 85287

Introduction: The objective of this investigation is to develop a prototype floodwater detection algorithm for Hyperion imagery. It will be run autonomously onboard the EO-1 spacecraft under the Autonomous Sciencecraft Experiment (ASE)[1-3]. This effort resulted in the development of two classifiers for floodwater, one of several classifier types that have been developed and will be uploaded to EO-1 in early 2004 in order to detect change related to transient processes such as volcanism, flooding, and ice formation and retreat [4].

Data: L0.5 Hyperion data were used to develop two floodwater classifiers: Avra Valley (AV) and Muddy Water (MW). For our investigation, we are most interested in seasonal flooding scenes, which include the following areas: (1) Avra Valley, Arizona (CAVSARP Recharge Facility [5]; ground-truthing field site; Fig. 1a), (2) Brahmaputra River, India, (3) Yukon Flats, Alaska (Fig. 2a), (4) Yellow River, China (Fig. 3a), (5) Chief Island, Botswana, Africa, and (6) Rio Tanquari Pantanal Swamps, Brazil. The advantage of using Hyperion data over some of the traditional satellite data is that it is hyperspectral with 242 spectral bands covering the 400 to 2400 nm spectral range at ~10-nm spectral resolution and 30-m spatial resolution. As a result, we are not limited by a few spectral bands and can utilize the full visible and near infrared (NIR) spectrum in classifier development for floodwater whose spectral signature can vary depending on its water composition.

Influences on water spectral signature: Water absorbs more in longer wavelength visible and near infrared radiation than in shorter visible wavelengths. Thus, water typically looks blue or blue-green due to a strong reflectance at these shorter wavelengths, and darker if viewed at red or NIR wavelengths. Suspended sediment in the upper layers of the water body will also allow better reflectivity and a brighter appearance of the water. The apparent color of the water will show a slight shift to longer wavelengths. Suspended sediment can be easily confused with shallow clear water, since these two conditions appear very similar. Sediments can also give water a dark brownish color (Fig.3a) or a milky color (as in the Yukon Flats scenes; Fig. 2a). Chlorophyll in algae absorbs more of the blue wavelengths and reflects the green, making some water appear more green in color when algae is present. Topography of the water surface (e.g., smooth, rough, floating materials, vegetation poking out of the water, etc.) can also lead to complications for water-related interpretation due to potential problems of specular reflection and other influences on color and

brightness. All these complications in the water spectral signature led us to develop a general non-scene specific flowchart (see Fig. 4), as a guideline in the floodwater classifiers development.

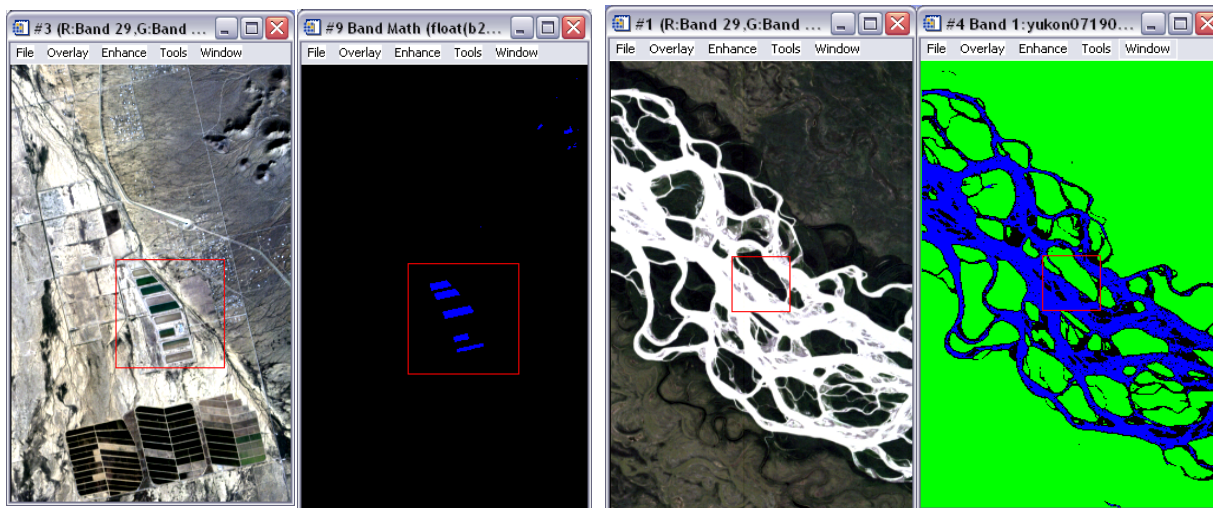
Approach: We began this effort by working with an existing band ratio developed from a scene that displayed the shield complex of Mt. Etna and nearby Mediterranean Sea, which discriminated the pristine volcanic landscape from the ocean water. In general, the optical properties of ocean water is largely affected by phytoplankton and its breakdown products [6]. Next, we tried to apply the Mt. Etna band ratio to the Avra Valley scenes where there is ground truth information. It did not perform well. This observation was determined to result from a difference in the water composition. The water from the CAVSARP recharge water [2] is influenced by ingredients more than phytoplankton. These may include dissolved organic matter, dead particulate organic matter, and/or inorganic matter (dissolved and particulate). Using this information, candidate bands were then picked where there is a significant separation between the water and the other spectra. Preferences were given to bands that were already chosen from other classifiers (in this case the cloud classifier). The new classifier performed optimally on the Avra Valley scenes (Fig. 1b). This Avra Valley classifier (AV) was then applied to other areas. AV worked relatively well for other areas such as Yukon Flats, Alaska (Fig. 2b), except in the case of the Yellow River where the water is laden with clay (Fig. 3b). For example, AV details water from erosional features such as streamlined bedforms in many of the scenes (Fig. 2b). For the Yellow River case a muddy water classifier (MW) was developed using the same methodology.

Description/Results: The criteria of using AV for floodwater detection is a ratio greater than 2.0 between radiance recorded in spectral bands 20 and 51 (0.549 and 0.864 μm). It works globally on river systems that have high flood probability and low sediment load. For MW, the criterion for floodwater detection is a ratio of less than 0.625 between band 85 and band 51 (0.993 and 0.864 μm). It works also globally on flood-prone river systems but with a relatively high sediment load. At these selected bands, there is a large separation between radiance reflected by floodwater and by the surrounding features. Pixels detected using both methods are color-coded blue in the classifier test runs (Figs 1b,2b,3b).

Summary and future work: The two floodwater classifiers are ready for upload to EO-1 and deployment for the 2004 ASE mission. Future investigations for floodwater detection would include using spectral information changes caused by other flood-related

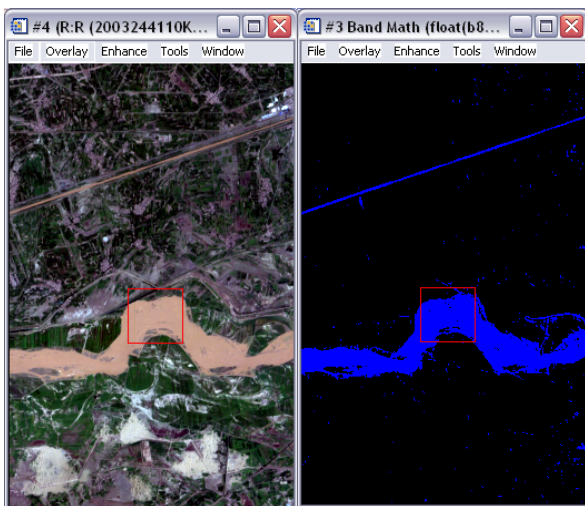
surface modification (e.g., topographic, geomorphic, and biologic), which could be indicative of flooding.

Acknowledgements: We are grateful to the City of Tucson and Tucson Water for their critical cooperation in this activity.

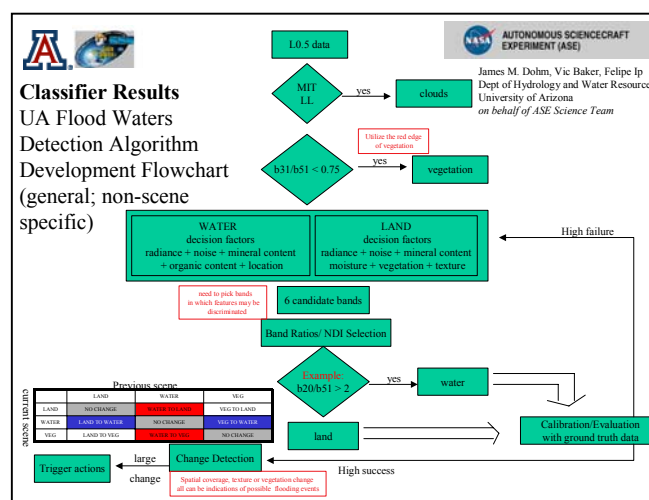


Figures 1a,b. Results for CAVSARP ground truth site.

Figures 2a,b. Results for Yukon Flats.



Figures 3a, b. Result for Yellow River scene.



Figures 4. Floodwater detection development flow chart.

References: [1] Chien, S. *et al.* (2001) I-SAIRAS, 6th Symp. on Artificial Intelligence, Robotics and Automation in: Space. Montreal, Canada, June 2001. [2] Chien, S. *et al.* (2004) Preliminary Results from the autonomous Sciencecraft Experiment, submitted to IEEE Conference [3] Davies A. G. *et al.* (2001) ASC Science Study Report, available from <http://ASE.jpl.nasa.gov>. [4] Davies, A. G. *et al.* (2004) Autonomous Sciencecraft Experiment (ASE) Operations on EO-1 2004, this volume. [5] Dohm *et al.* (2004), this volume. [6] Pozdnyakov, D. *et al.* (2003) Colour of Inland and Coastal Waters.